7. G. I. Barenblatt, I. G. Bulina, V. N. Kalashnikov, and N. M. Kolinichenko, Zh. Prikl. Mekh. Tekh. Fiz., No. 6 (1966).
8. V. I. Klenin, N. K. Kolnibolotchuk, and S. Ya. Frenkel', Vysokomol. Soedin., B15, 389 (1973).
9. A. Peterlin, Nature, 227, No. 5258 (1970).

EFFECT OF SURFACTANT ON BUBBLE MOTION CLOSE TO A SOLID WALL

I. E. Shchekin

UDC 541.183:532.529.6

Numerical analysis is used to study the effect of surfactants on the parameters of gas-bubble motion close to a solid wall under the influence of abrupt pressure change at infinity.

The study of gas-bubble motion close to a solid wall in liquids containing dissolved surfactant is of great interest for the design of chemical-engineering apparatus for a number of important liquid-extraction processes and also in connection with the production technology for various solvents.

The present work gives the results of a numerical investigation of gas-bubble motion close to a solid wall in an incompressible liquid containing surfactant, under the influence of an abrupt pressure change at infinity.

Consider a bubble of radius R situated a distance x from the wall; the bubble pulsates and moves toward the wall with velocity $\dot{x}$. This bubble motion may be described by Lagrange equations [1]

$$\frac{d}{dt}\frac{\partial T}{\partial \dot{x}} - \frac{\partial T}{\partial x} = F_x, \quad \frac{d}{dt}\frac{\partial T}{\partial \dot{R}} - \frac{\partial T}{\partial R} = F_R, \tag{1}$$

where T is the kinetic energy of the liquids, calculated from the potential and its derivatives at the boundary surfaces by the formula

$$T = -\frac{\rho}{2}\iint_S \varphi \frac{\partial \varphi}{\partial n} dS.$$

The velocity-field potential φ satisfies the Laplace equation with the following boundary conditions

$$-\frac{\partial \varphi}{\partial n}\Big|_{r=R} = \dot{R} - \dot{x}\cos\theta, \quad -\frac{\partial \varphi}{\partial n} = 0 \text{ at the wall}, \quad (\operatorname{grad}\varphi)_\infty = 0. \tag{2}$$

Using the method outlined in [2-4] to find the function φ satisfying the boundary conditions in Eq. (2), the liquid kinetic energy for the bubble close to the solid wall is given, retaining terms of order up to ε^3, by the expression

$$T = 2\pi\rho R^3[(1/3 - 1/8\,\varepsilon^3)\dot{x}^2 + (2 + \varepsilon)\dot{R}^2 - 1/2\varepsilon^2\dot{x}\dot{R}]. \tag{3}$$

The system in Eq. (1) may be used in the case when the velocity field of the real liquid deviates slightly from the corresponding velocity field of an ideal liquid. It was shown in [5] that this condition is satisfied for a liquid with $Re \gg 1$. Assume that the surfactant does not have a great effect on the hydrodynamics close to the bubble surface; then, according to [6], the generalized force F_x is given by the expression

$$F_x = 12\pi\mu R\dot{x} - 1.15\lambda R^* T_1 R\Gamma_0. \tag{4}$$

When the surfactant concentration is small and adsorption is far from saturation [7]

$$\lambda = \frac{\Gamma_0}{RC_0}\left(\frac{|\dot{x}|R}{D}\right)^{1/2}. \tag{5}$$

Substituting Eq. (5) into Eq. (4) gives

$$F_x = 12\pi\mu R\dot{x} - 1.15R^* T_1 \Gamma_0^2 C_0^{-1}\left(\frac{|\dot{x}|R}{D}\right)^{1/2}. \tag{6}$$

Sukhumsk Branch of the Acoustic Institute, Academy of Sciences of the USSR. Translated from Inzhenerno-Fizicheskii Zhurnal, Vol. 34, No. 1, pp. 84-88, January, 1978. Original article submitted October 6, 1976.

0022-0841/78/3401-0055$07.50

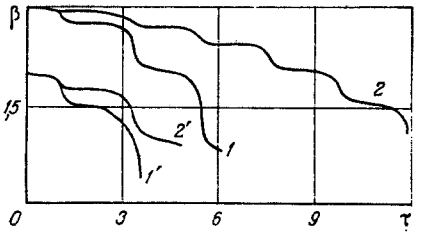

Fig. 1. Dependence of bubble displacement $\beta = x/R_0$ on time $\tau = (t/R_0)(P_0/\rho)^{1/2}$ for $x_0/R_0 = 3$ (1, 2) and $x_0/R_0 = 2$ (1', 2'): 1, 1') in the absence of surfactant; b) with surfactant.

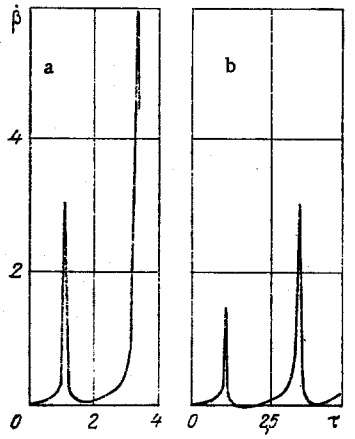

Fig. 2

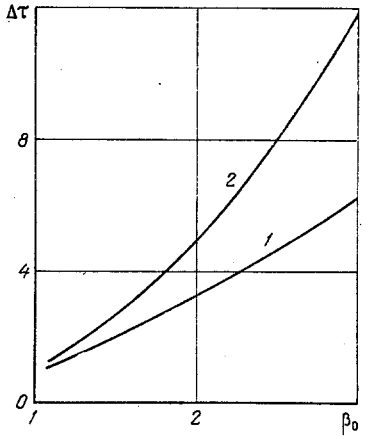

Fig. 3

Fig. 2. Dependence of velocity of bubble $\dot{\beta} = (dx/dt)(\rho/P_0)^{1/2}$ on time $\tau = (t/R_0)(P_0/\rho)^{1/2}$ for $\beta_0 = x_0/R_0 = 2$: a) in the absence of surfactant; b) with surfactant.

Fig. 3. Time $\Delta\tau = (\Delta t/R_0)(P_0/\rho)^{1/2}$ for the bubble to reach the solid wall as a function of the initial distance from the wall $\beta_0 = x_0/R_0$: 1) without surfactant; 2) with surfactant.

The generalized force F_R is given by the expression

$$F_R = 8\pi R^2 \left(P_r - P_0 - \frac{2\sigma}{R} - 4\mu \frac{\dot{R}}{R} \right).$$

The surface tension σ is related to the adsorbed-material distribution Γ_0 over the bubble surface by the Gibbs equation [7]

$$\sigma = \sigma_0 - R^* T_1 \Gamma_0.$$

Then

$$F_R = 8\pi R^2 \left(P_r - P_0 - \frac{2\sigma_0}{R} + \frac{2R^* T_1 \Gamma_0}{R} - 4\mu \frac{\dot{R}}{R} \right). \tag{7}$$

Substituting Eqs. (3), (4), and (7) into Eq. (1) leads to a system of two differential equations describing the radial and translational motion of the bubble close to a solid wall in the presence of surfactant:

$$\begin{aligned} &\eta\ddot{\eta}(1 + \varepsilon/2) + (3/2 + \varepsilon)\dot{\eta}^2 - 1/2\varepsilon^2\dot{\eta}\dot{\beta} - 1/8\varepsilon^2\eta\ddot{\beta} - 1/4\dot{\beta}^2 + 1 - \\ &- \delta/\eta^4 + E/\eta - 2\overline{R}^* \overline{T}_1 \overline{\Gamma}_0 \eta^{-1} + 4M\dot{\eta}\eta^{-1} = 0, \\ &(1 + 3/8\varepsilon^3)\eta\ddot{\beta} + (3 + 9/4\varepsilon^3)\dot{\eta}\dot{\beta} - 9/4\varepsilon^2\dot{\eta}^2 - 3/4\varepsilon^2\eta\ddot{\eta} - \\ &- 9/16\varepsilon^4\dot{\beta}^2 - 9M\dot{\beta}\eta^{-1} + 0{,}8625 \frac{\overline{R}^* \overline{T}_1 \overline{\Gamma}_0 |\dot{\beta}|^{1/2}}{\overline{C}_0 \overline{D}^{1/2} \eta^{3/2}} = 0, \end{aligned} \tag{8}$$

$$\eta = R/R_0,\ \beta = x/R_0,\quad \dot{\eta} = \frac{dR}{dt}\left(\frac{\rho}{P_0}\right)^{1/2},\ \dot{\beta} = \frac{dx}{dt}\left(\frac{\rho}{P_0}\right)^{1/2},$$

$$\ddot{\eta} = \frac{d^2R}{dt^2}\frac{R_0\rho}{P_0},\ \ddot{\beta} = \frac{d^2x}{dt^2}\frac{R_0\rho}{P_0},\ \tau = \frac{t}{R_0}\left(\frac{P_0}{\rho}\right)^{1/2},$$

$$\delta = P_{g0}/P_0,\ \bar{T}_1 = T_1/T_0,\ \bar{R}^* = \frac{R^*T_0N}{P_0R_0^3},\ \bar{\Gamma}_0 = \frac{\Gamma_0R_0^2}{N},$$

$$\bar{C}_0 = \frac{C_0R_0^3}{N},\ \bar{D} = \frac{D}{R_0}\left(\frac{\rho}{P_0}\right)^{1/2},\ E = \frac{2\sigma}{P_0R_0},\ M = \frac{\mu}{R_0\sqrt{P_0\rho}}.$$

In obtaining Eq. (8), it is assumed that the gas in the bubble is compressed adiabatically, $\gamma = 4/3$.

Numerical solution of Eq. (8) was carried out on a computer by the Runge–Kutta method. The initial conditions used in solving Eq. (8) correspond to the assumptions that initially the bubble (radius $R_0 = 0.0001$ m) is at rest; that the difference between the pressure at infinity and that inside the bubble $\Delta P = P_0 - P_{g0} = 0.9 \cdot 10^5$ N/m^2 for $t = 0$, $\eta_0 = 1$, $\beta = \beta_0$, $\dot{\eta} = 0$, $\dot{\beta} = 0$; and that the bubble is moving in an aqueous solution of amyl alcohol at 18°C (diffusion coefficient $D = 0.88 \cdot 10^{-9}$ m^2/sec; $\Gamma_0/C_0 = 3.55 \cdot 10^{-4}$ [4]; $C_0 = 0.01$ M).

As an example, Figs. 1 and 2 show results for the displacement (Fig. 1) and velocity (Fig. 2) of the bubble as a function of time, with and without additions of surfactant, for various initial distances from the wall.

Analysis of the results shows that the bubble displacement and its velocity toward the wall are significantly different before and after the addition of surfactant. Thus, it is evident from the curves (for $\beta_0 = 2$) that the addition of surfactant halves the maximum bubble velocity toward the wall.

In the present case, the bubble reaches the wall from any initial distance, although several compression and expansion cycles may be required.

The existence of maxima and minima in the translational bubble velocity toward the wall (Fig. 2) may be explained by means of the momentum-conservation law $m\dot{x} = \text{const}$, where m is the associated mass of liquid, equal to $(2/3)\pi\rho R^3$ for translational bubble motion.

Hence it is evident that, on compression to the minimum size, the translational bubble velocity increases and reaches a maximum, while on expansion to the maximum size the bubble velocity decreases and reaches a minimum. The increase in the maximum translational velocity observed with increase in time is explained by a decrease in the bubble–wall distance and, hence, an increase in the attractive forces between the bubble and the wall. Fluctuations in the translational bubble velocity lead to a certain nonmonotonic dependence $\beta(\tau)$ (Fig. 1).

The time for the bubble surface to reach the solid wall is shown in Fig. 3 as a function of the initial distance, with (curve 2) and without (curve 1) addition of surfactant. It is evident from these curves that the change in the time required for the bubble to reach the solid wall that results from the addition of surfactant increases with increase in the initial distance from the wall.

Note that as is evident from Eq. (6), increase in parameters such as Γ_0 and T_1 or decrease in C_0 is accompanied by an increase in the retarding forces due to the surfactant and hence to a decrease in the translational bubble velocity toward the solid wall.

These results indicate that surfactant has a significant effect on bubble motion toward a solid wall, even at low surfactant concentrations.

NOTATION

R_0, R, bubble radius at initial and present times; x_0, x, initial and present distance from bubble center to wall; T, kinetic energy of liquid; μ, dynamic viscosity of liquid; R*, universal gas constant; T_1, temperature; Γ_0, equilibrium surface concentration of adsorbed material; λ, parameter defined by Eq. (5); C_0, concentration of material dissolved in liquid; D, diffusion coefficient; σ_0, surface tension in the absence of surfactant; σ, surface tension with surfactant present; $P_g = P_{g0}(R_0/R)^{3\gamma}$, gas pressure in bubble; P_{g0}, gas pressure in bubble when $R = R_0$; P_0, pressure in liquid; M, dimensionless viscosity; γ, adiabatic coefficient; t, time; τ, dimensionless time; $\Delta\tau$, time for bubble surface to reach solid wall; $\delta = P_{g0}/P_0$, relative gas content; N, number of moles of material; r, θ, polar coordinates.

LITERATURE CITED

1. L. M. Milne-Thomson, Theoretical Hydrodynamics, Macmillan (1968).
2. O. V. Voinov and A. G. Petrov, Izv. Akad. Nauk SSSR, Mekh. Zhidk. Gaza, No. 5 (1971).
3. G. N. Kuznetsov and I. E. Shchekin, Akust, Zh., 18, No. 4 (1972).
4. Yu. L. Levkovskii, Akust. Zh., 20, No. 1 (1974).
5. A. M. Golovin, Zh. Prikl. Mekh. Tekh. Fiz., No. 6 (1967).
6. A. G. Petrov, Teor. Osn. Khim. Tekh., 4, No. 3 (1970).
7. V. A. Naumov, Colloid Chemistry [in Russian], Leningrad (1932).

HEAT TRANSFER INSIDE A ROTATING RECTANGULAR CAVITY

V. K. Shchukin

UDC 536.24

The qualitative liquid-flow pattern is considered for a rotating rectangular cavity in the case of heat transfer in a direction parallel to the axis of rotation; calculational relations describing the heat transfer are obtained.

Calculations of the temperature state of rotating machine parts require information on heat-transfer coefficients in channels and cavities. One type of rotating cavity is shown in Fig. 1: The cavity is in the form of a rectangular closed parallelepiped, through which there is heat transfer in a direction parallel to the axis of rotation. The liquid motion in such a cavity is determined by centrifugal and Coriolis forces.

The field due to the centrifugal mass forces is inhomogeneous, because of the change in the liquid density in the thermal boundary layer near the heat-transfer surface and also as a result of the variation in the inertial centrifugal acceleration over the radius of rotation.

The variation in liquid density in the direction normal to the heat-transfer surface gives rise to radial displacement of the liquid and leads to the development of circulation in opposite directions in the two halves of the cavity. The directions of the circulatory motion are indicated on the side surface of the cavity in Fig. 1.

The liquid motion near the cooled wall occurs in a positive pressure gradient, while close to the heated wall there is a negative pressure gradient.

The Coriolis acceleration vector lies in the cross-sectional plane, and varies in magnitude in accordance with the velocity of radial displacement of the liquid. The distribution of the radial velocity and the direction of the Coriolis force in the cross section are indicated on the front wall of the cavity in Fig. 1. This Coriolis-force distribution may give rise to rotational motion of the liquid, leading to changes in the heat-transfer conditions. The direction of motion is shown in Fig. 1.

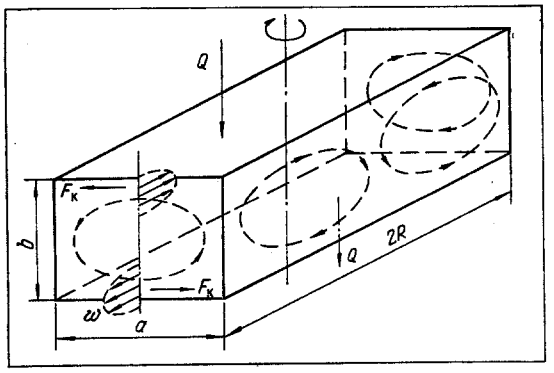

Fig. 1. Diagram of rotating cavity.

Translated from Inzhenerno-Fizicheskii Zhurnal, Vol. 34, No. 1, pp. 89-93, January, 1978. Original article submitted November 23, 1976.

0022-0841/78/3401- 0058 $07.50